JOURNAL OF MATERIALS SCIENCE 26 (1991) 3433–3437

Crystallization kinetics of bulk amorphous $Se_{80-x}Sb_xTe_{20}$

R. M. MEHRA, G. KAUR, P. C. MATHUR
Department of Electronic Science, University of Delhi South Campus, Benito Juarez Road, New Delhi 110021, India

Crystallization kinetics of the $Se_{80-x}Sb_xTe_{20}$ ($0 \leqslant x \leqslant 9$) alloys have been studied using differential scanning calorimetry. The activation energies for the glass transition and that for crystallization have been determined from the heating rate dependence of the glass transition temperature and the peak crystallization temperature. The results have been analysed using the modified Kissinger's and Matusita's equations for the non-isothermal crystallization of materials. The variation of glass transition temperature with composition suggests that a small amount of Sb ($\leqslant$ 4 at %) leads to an increase in the chain length of Se–Te, whereas further increase in Sb atomic per cent increases the number of Se–Te chains in the alloys.

1. Introduction

The Se–Sb–Te system has wide application as a photo-receptor in xerography and in switching and memory devices [1]. It has been found that the Se–Sb–Te system shows memory-type switching and that the structure and electrical properties of glass are considerably modified by the addition of Sb. A systematic investigation of thermal stability and crystallization kinetics of the Se–Sb–Te system is reported here for different Se:Sb ratios, keeping the Te content at 20 at %. Calorimetric measurements were used to study the dependence of the glass transition temperature, T_g, the crystallization temperature, T_c, and the peak temperature of crystallization, T_p, on composition and heating rate. From the heating rate dependence of T_g and T_p, the activation energy, E_t, for the glass transition and for crystallization, E_c, have been evaluated. Crystallization studies were made under non-isothermal conditions with the samples heated at several uniform rates. The results of crystallization are discussed on the basis of Kissinger's approach and Matusita's modified expression for non-isothermal crystallization.

2. Experimental procedure

Bulk samples of the $Se_{80-x}Sb_xTe_{20}$ ($0 \leqslant x \leqslant 9$) were prepared by the melt-quenching technique. Appropriate mixtures of 99.999% purity elements were sealed off in a vacuum of 10^{-5} torr (1 torr = 1.333×10^2 Pa) in quartz ampoules (4 mm diameter) and placed in a microprocessor-controlled programmable working furnace (model 73211, Harrop, USA) at 650 °C for 30 h. The furnace was constantly rocked to ensure proper mixing of the constituents. The melt was then rapidly quenched in ice–water. Quenched samples were removed from the ampoule by dissolving the ampoule in a mixture of $HF + H_2O_2$ for about 24 h.

DSC thermograms for various compositions of the samples quenched from 650 °C were obtained with a Dupont DSC 1090 calorimeter in the temperature range 50–300 °C to obtain the T_g and T_p of the samples at various heating rates (5–50 °C min^{-1}). The samples (2–3 mg) in powder form were placed in standard aluminium pans and scanned over a temperature range of about 250 °C. T_g was taken as the temperature corresponding to the intersection of the two linear portions adjoining the transition elbow in the DSC traces. The fraction X crystallized at any temperature, T, is given as $X = A_T/A$ where A is the total area of the exotherm between temperature T_1 where crystallization just begins and the temperature T_2 where the crystallization is completed (Fig. 1), A_T is the area between T_1 and T as shown by the hatched portion in Fig. 1.

3. Results and discussion

3.1. Compositional dependence of T_g, E_t, T_p and E_c

The glass transition temperature was found to increase with the addition of small amount of Sb (< 4 at %) (Fig. 2). However, a further increase in the Sb content reduced the glass transition temperature. The results are shown in Table I. It is observed that the values of T_g and T_p shift to higher temperatures with increasing heating rates for all the samples. Fig. 3 represents DSC thermograms for the $Se_{76}Sb_4Te_{20}$ sample.

The empirical relation [2] $T_g = A + B \log \alpha$, where A and B are constant and α is the heating rate, holds good for all the samples. Plots of T_g versus $\log \alpha$ are shown in Fig. 4. The value of B is found to be different for different glass compositions, indicating that Se–Sb–Te alloy undergoes structural changes for different Sb concentrations, because the value of B is an

0022-2461/91 $03.00 + .12

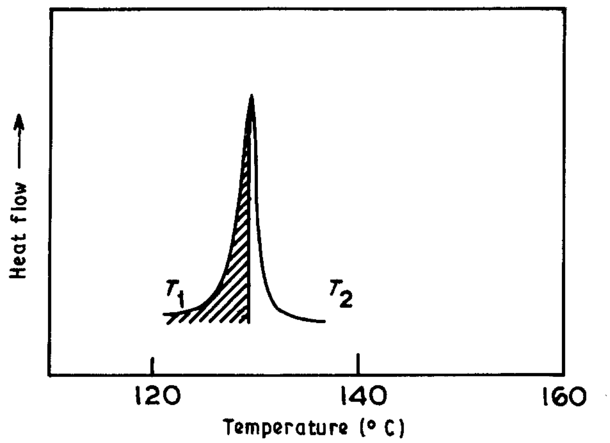

Figure 1 A typical DSC crystallization exotherm obtained for $Se_{76}Sb_4Te_{20}$ at a heating rate of 20 °C min^{-1}.

TABLE I Variation of T_g and T_p with heating rate

Material	T_g(K)			T_p(K)		
	Heating rate (°C min^{-1})			Heating rate (°C min^{-1})		
	5	10	20	5	10	20
$Se_{80}Te_{20}$	331	337	341	404	410	418
$Se_{76}Sb_4Te_{20}$	369	376	382	411	416	422
$Se_{74}Sb_6Te_{20}$	360	363	368	402	407	415
$Se_{71}Sb_9Te_{20}$	347	352	358	397	404	413

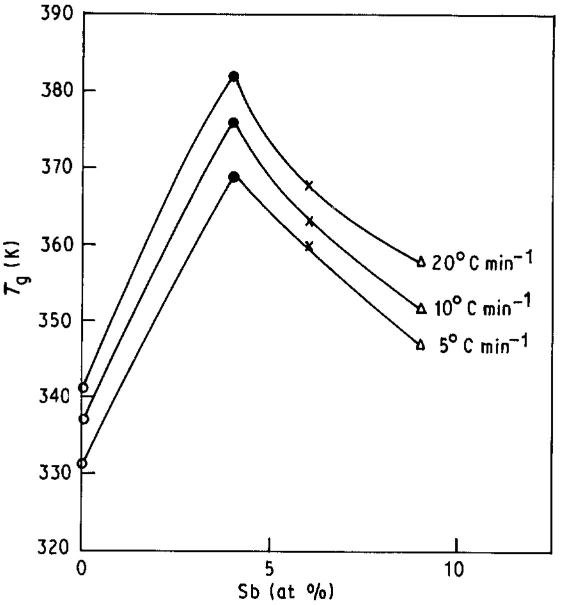

Figure 2 Variation of T_g with composition for bulk amorphous $Se_{80-x}Sb_xTe_{20}$ at different heating rates.

indication of the response of configurational changes within the glass transition region [2]. The values of *B* listed in Table II lie in the range 9–19. The structure of the amorphous Se–Te system prepared by quenching from the melt is regarded as a mixture of eight-membered rings, Se_6Te_2 mixed rings and the SeTe

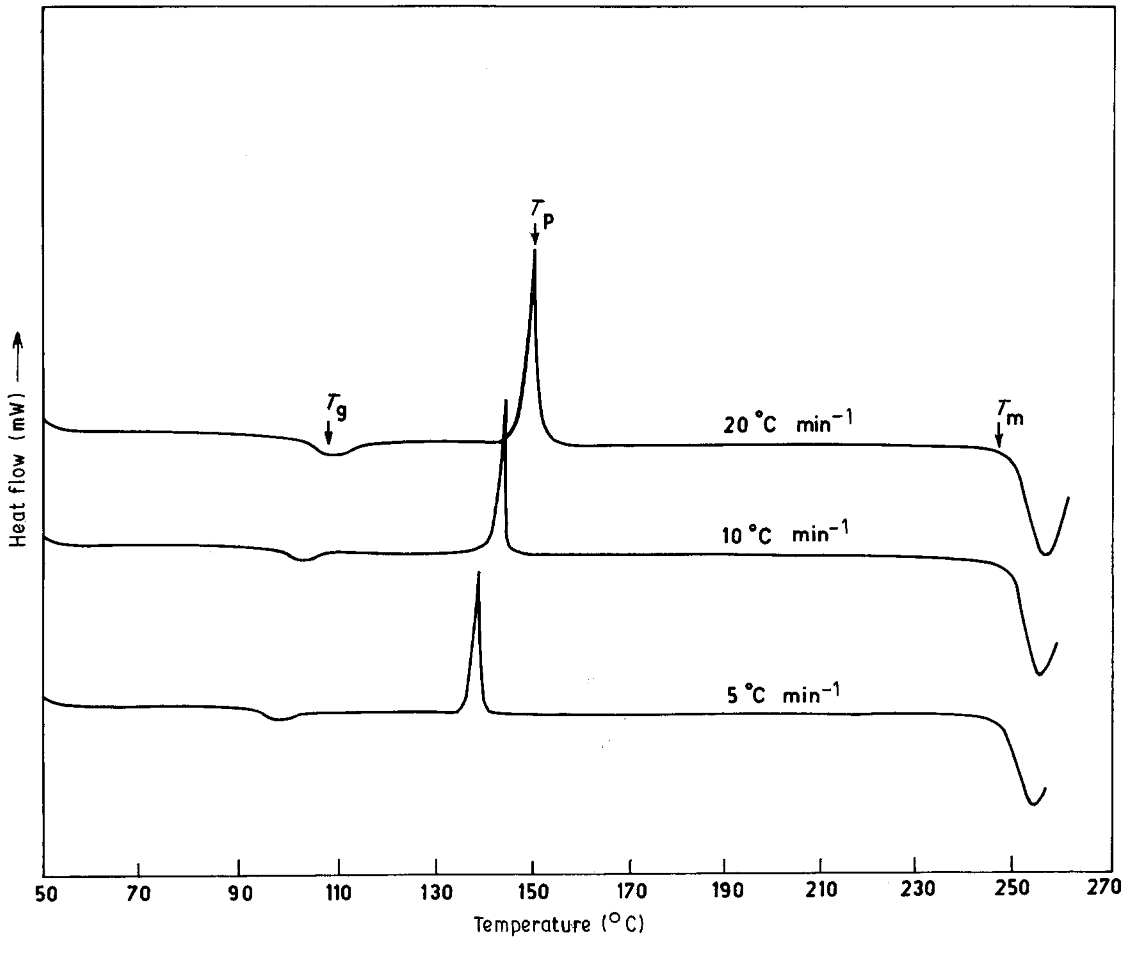

Figure 3 The glass transition temperature and the peak crystallization temperature at different heating rates for $Se_{76}Sb_4Te_{20}$.

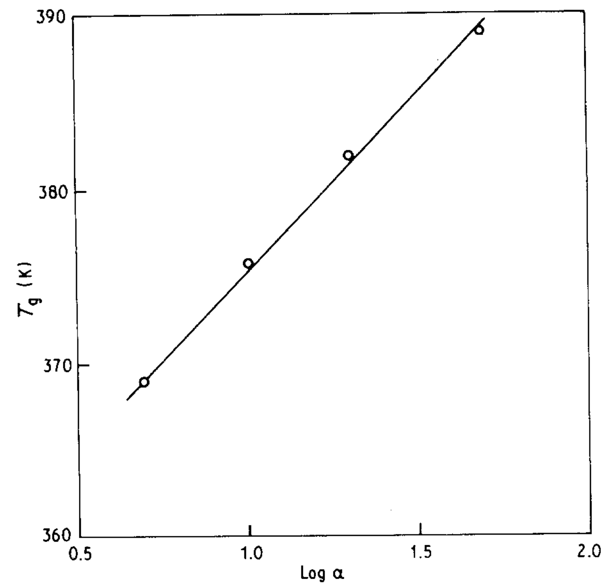

Figure 4 T_g versus log α for $Se_{76}Sb_4Te_{20}$.

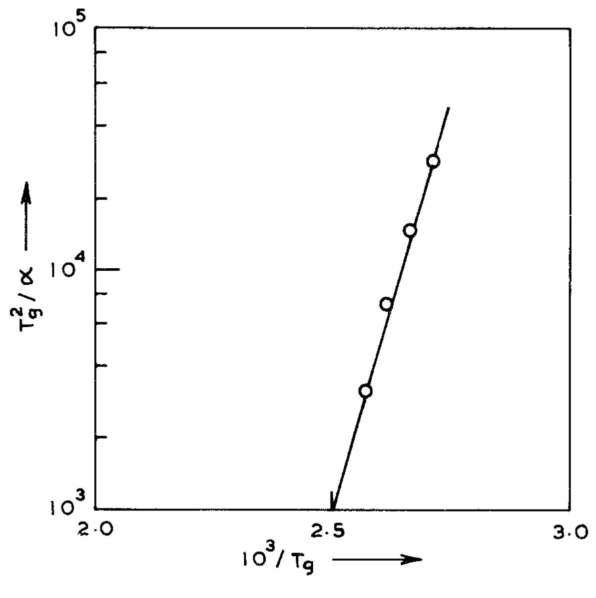

Figure 5 Log (T^2/α) versus $1/T_g$ for $Se_{76}Sb_4Te_{20}$ for heating rates up to 50 °C min^{-1}.

chains. Strong covalent bonds exist between the atoms in the rings whereas inbetween the chains, the Van der Waals forces are dominant. The addition of a small amount of Sb ($\leqslant$ 4 at %) to the SeTe system leads to cross-linking of the chains to a small extent, hence increasing the chain length which leads to an increase in the T_g of the system. Further, addition of Sb leads to an increase in the number of chains which results in a decrease of the T_g of the system.

The activation energy, E_t, for the glass transition is calculated using Kissinger's formula [3]

$$\ln(T_g^2/\alpha) + \text{constant} = E_t/RT_g \qquad (1)$$

Plots of $\ln(T_g^2/\alpha)$ versus $1/T_g$, shown in Fig. 5, are found to be linear for the entire heating rate range for all the samples. Values of E_t for different compositions of the samples are listed in the Table II. Activation energy, E_t, for the glass transition is found to vary from 28.55–35.18 Kcal mol^{-1} for different samples.

The value of T_p obtained from the same thermograms for different heating rates and composition are also listed in Table I. The activation energy for crystallization, E_c, has been obtained using the modified Kissinger equation [4–10].

$$\ln(\alpha^n/T_p^2) = -mE_c/RT_p + \ln K \qquad (2)$$

where K is a constant containing factors depending on the thermal history of the samples, and n and m are constants having values between 1 and 4 depending on the morphology of the growth. The value of mE_c/n was determined from the slope of the curves ln α versus $1000/T_p$, as shown in Fig. 6. The values of mE_c/n are also listed in Table II.

For the non-isothermal crystallization, Matusita *et al.* [8] have given the expression

$$\ln[-\ln(1 - X)] = -n\ln\alpha - 1.052\frac{mE_c}{RT} + \text{constant} \qquad (3)$$

where X is the volume fraction of crystals precipitated in the glass heated at uniform rate, E_c is the activation energy for crystallization, R is the gas constant. The value of n (Table I) is obtained from the slope of the $\ln[-\ln(1 - X)]$ versus ln α curve. Because no particular heat treatment was given before the thermal analysis run to nucleate the samples, m is taken to be equal to $n - 1$ [4]. Value of n is found to be nearly 4 for all samples.

The value $n = 4$ which gives $m = 3$ suggests that bulk nucleation in three dimensions is dominant (Table III) [4]. The values of E_c, evaluated using these values of m and n, are given in Table II, column 7.

The value of mE_c (Table II) is obtained from the slope of the $\ln[-\ln(1 - X)]$ versus $1000/T_p$ curve, Fig. 7. The curve is a straight line for most of the temperature range but shows a break at higher temperatures, which is attributed to the saturation of nucleation sites in the final stages of crystallization [11, 12] or to restriction of crystal growth by the small size of the particles [13]. In such cases the analysis is restricted to the initial linear region extending over

TABLE II Parameters determined from the heating rate data on $Se_{80-x}Sb_xTe_{20}$ samples

Material	B	E_t (kcal mol^{-1})	mE_c/n (kcal mol^{-1})	n	m	E_c (kcal mol^{-1})	mE_c (kcal mol^{-1})	E_c (kcal mol^{-1})
$Se_{80}Te_{20}$	14.28	28.55	27.19	4.16	3	37.7	91.25	30.41
$Se_{76}Sb_4Te_{20}$	18.3	35.18	33.16	4.17	3	46.09	226.1	75.33
$Se_{74}Sb_6Te_{20}$	13.33	35.18	25.15	4.28	3	35.88	173.15	57.71
$Se_{71}Sb_9Te_{20}$	9.6	32.67	21.17	4.45	3	31.40	75	25

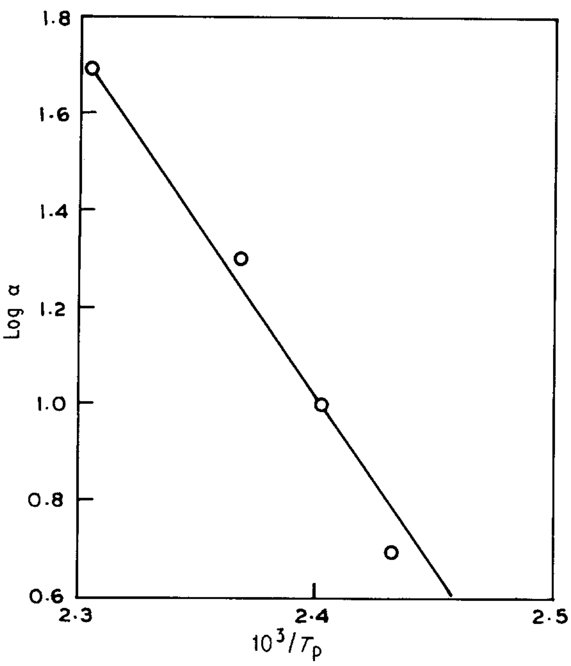

Figure 6 Ln α versus $10^3/T_p$ for $Se_{76}Sb_4Te_{20}$ glass.

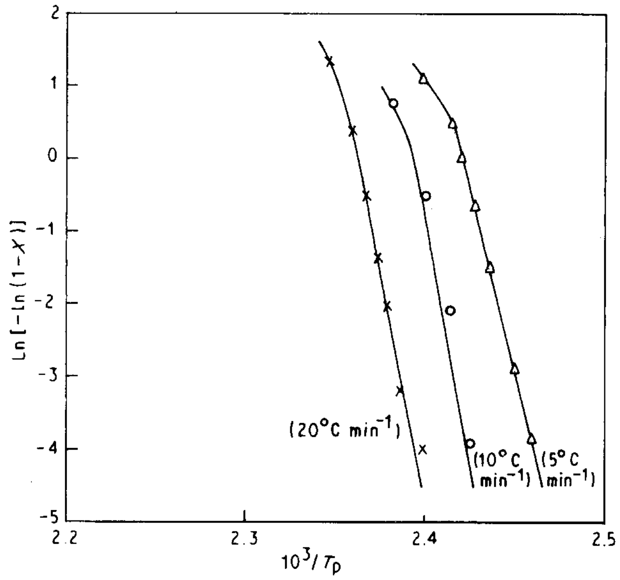

Figure 7 Ln [− ln (1 − X)] versus $10^3/T_p$ for $Se_{76}Sb_4Te_{20}$ at the different heating rates indicated.

TABLE III Values of n and m for various crystallization mechanisms

Mechanism	n	m
Bulk nucleation:		
three-dimensional growth	4	3
two-dimensional growth	3	2
one-dimensional growth	2	1
Surface nucleation	1	1

a larger range. E_c is again obtained using the value of m and mE_c. These values are also given in Table II, column 9. It is evident from the results that the values of E_c (columns 7 and 9) obtained by the two methods are not the same. The reason for this discrepancy is not clear; however, such results are also obtained in the case of $Li_2O–2SiO_2$ glass [7].

3.2. Thermal stability and the ease of glass formation

The value of $T_c - T_g$ is found to decrease with increasing Sb concentration, which indicates a decrease in the thermal stability of the glasses [14] with increasing Sb content. The glass-forming tendency is evaluated using the relation [15]

$$K_{gl} = \frac{T_c - T_g}{T_m - T_c} \qquad (4)$$

K_{gl} varies from 0.54–0.29 (Table IV) which also indicates that the glasses with higher Sb content are difficult to form compared to those with lower Sb content. An increased crystalline nature of the samples with higher Sb content is also indicated by the presence of sharp peaks in the X-ray diffractograms of the sample containing 10 at % Sb, as shown in Fig. 8.

4. Conclusion

In the present work, a systematic investigation of the thermal stability and crystallization kinetics of the $Se_{80-x}Sb_xTe_{20}$ $(0 \leqslant x \leqslant 9)$ system has been done.

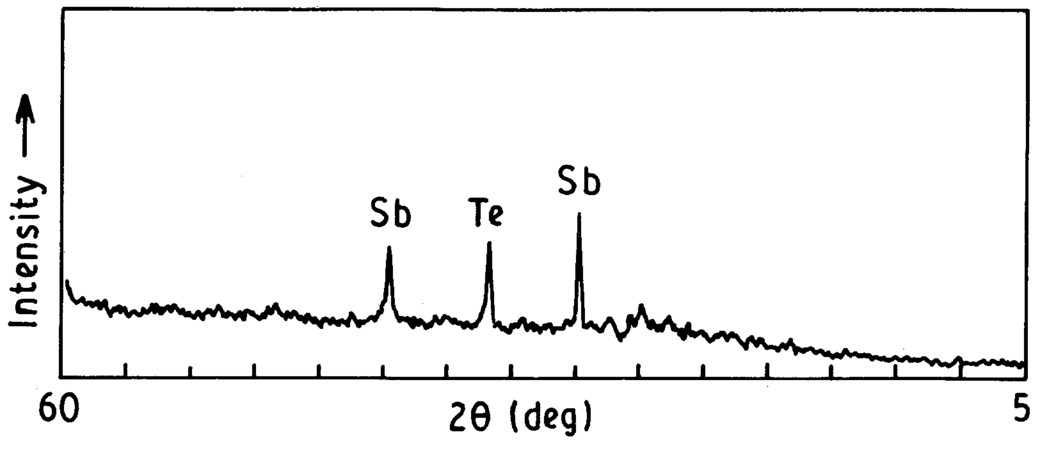

Figure 8 X-ray diffractogram of the $Se_{70}Sb_{10}Te_{20}$ sample showing the polycrystalline nature of the sample.

TABLE IV Parameters determined for the glass-forming tendency of $Se_{80-x}Sb_xTe_{20}$ at a heating rate of 10 °C min^{-1}

Material	T_g (K)	T_c (K)	T_m (K)	$T_c - T_g$ (K)	$T_m - T_c$ (K)	K_{gl}
$Se_{80}Te_{20}$	337	402	521	65	119	0.54
$Se_{76}Sb_4Te_{20}$	376	413	523	37	110	0.33
$Se_{74}Sb_6Te_{20}$	363	402	523	39	121	0.32
$Se_{71}Sb_9Te_{20}$	352	391	522	39	131	0.29

From the heating rate dependence of T_g and T_p, the activation energy for the glass transition and for crystallization have been evaluated. The results are discussed on the basis of Kissinger's approach and Matusita's modified expression for non-isothermal crystallization. It has been suggested that the addition of Sb ($\leqslant 4$ at %) increases the chain length of Se–Te resulting in an increase of the T_g of the system, whereas further increase in Sb at % leads to a breaking of the chains and the formation of a large number of smaller chains results in a decrease in T_g. It is also concluded that the Se–Te–Sb system shows a reduced tendency towards glass formation at higher Sb at %.

References

1. A. ONOZUKA and O. ODA, *J. Non-Cryst. Solids* **103** (1988) 289.
2. M. LASOCKA, *Mater. Sci. Engng* **23** (1976) 173.
3. H. E. KISSINGER, *J. Res. Nat. Bur. Stand.* **57** (1956) 217.
4. K. MATUSITA and S. SAKKA, *Phys. Chem. Glasses* **20** (1979) 81.
5. D. R. MACFARLANE, M. MATECKI and M. POULAIN, *J. Non-Cryst. Solids* **64** (1984) 351.
6. K. MATUSITA and S. SAKKA, *ibid.* **38–39** (1980) 741.
7. *Idem., Bull. Inst. Chem. Res. Kyoto Univ.* **59** (1981) 159.
8. K. MATUSITA, T. KONATSU and R. YOKOTA, *J. Mater. Sci.* **19** (1984) 291.
9. A. MOROTTO, S. SAIELLO and A. BURI, *J. Non-Cryst. Solids* **57** (1983) 473.
10. K. MATUSITA and S. SAKKA, *Therm. Chim. Acta* **33** (1979) 351.
11. J. COLEMENERO and J. M. BARANDIARAN, *J. Non-Cryst. Solids* **30** (1978) 263.
12. P. DUHAJ, D. BARANCOK and A. ONDRJKA, *ibid.* **21** (1976) 411.
13. R. F. SPEYER and S. H. RISBUD, *Phys. Chem. Glasses* **24** (1983) 26.
14. S. MAHADEVAN, A. GIRIDHAR and A. K. SINGH, *J. Non-Cryst. Solids* **88** (1986) 11.
15. A. HRUBY, *Czech. J. Phys. B* **22** (1972) 1187.

Received 19 April
and accepted 6 November 1990